Effect of Soil Slope on Lateral Response of Piled Raft Foundations in Cohesive Soil

S. Lateh[1], T. Chub-Uppakarn[1]*, P. Jongpradist[2], T. Chompoorat[3], S. Swasdi[1], and W. Srisakul[4]
[1]*Department of Civil and Environmental Engineering, Prince of Songkla University, Hat yai, Songkhla, Thailand*
[2]*Department of Civil Engineering, King Mongkut's University of Technology Thonburi, Bangkok, Thailand*
[3]*Department of Civil Engineering, University of Phayao, Phayao, Thailand*
[4]*Department of Engineering Technology, Faculty of Engineering and Technology, Rajamangala University of Technology Srivijaya, Trang, Thailand*
**E-mail: tanan.c@psu.ac.th*

ABSTRACT: The advantages of the piled raft foundations system over conventional pile group foundations have been demonstrated in previous studies. In a pile raft foundation, the raft load capacity is extensively investigated in level ground conditions; its behaviour in a soil slope is limited. In the present study, three-dimensional finite element analyses using PLAXIS 3D software were performed to examine the effect of the soil slope on the lateral response of the piled raft foundation. The study showed that the lateral capacity of piled raft foundations decreases when installed within a certain distance (less than 8 times the pile diameter) from a slope. Furthermore, the enormous effect of slope occurs at distances nearer than 4D. Despite a decrease in lateral capacity when installed near slopes, the effect on the piles is insignificant, especially the rear piles. As a result, the distance between the piled raft foundations and the slope is a key factor that needs to be considered to improve design guidance to reduce construction costs.

KEYWORDS: Piled raft foundation, Soil slope, Lateral resistance, 3D Finite element, and Raft load sharing.

1. INTRODUCTION

Foundations in civil engineering often encounter complex challenges, particularly when situated atop natural or artificial slopes. These foundational structures must contend with both vertical and lateral loads, emanating from various sources such as wind, earthquakes, moving traffic, and earth pressure (Jamsawang et al., 2021; Likitlersuang et al., 2019). In the case of onshore structures, this lateral load can be 10 - 15% of the vertical loads, and it exceeds about 30% of the vertical load in the case of coastal structures (Deb and Pal, 2019). Consequently, the design considerations for such structures frequently prioritize lateral loading effects.

The adoption of pile foundations in slope environments introduces additional complexities, notably in terms of lateral load capacity. Nevertheless, if pile foundations are adopted, the lateral capacity of the piles will be reduced as those piles are installed closer to the slopes due to the reduction of passive resistance to be mobilized in front of piles. The minimum distance from the slope crest, unaffected by lateral responses, varies based on soil properties, depth, and slope angle (Georgiadis and Georgiadis, 2010; Jiang et al., 2018; Mezazigh and Levacher, 1998; Nimityongskul et al., 2018). For instance, piles in cohesive soil, revealing diminished lateral capacity when piles were positioned closer than eight times the diameter (8D) from a slope (Nimityongskul et al., 2018). The maximum lateral capacity decreased by 20% and 30% when the piles were installed at the distance 4D and 2D, respectively, from a slope. Therefore, under slope conditions, larger piles, whether in size or number, are needed to ensure the serviceability of the foundations.

Piled raft foundations have emerged as a prominent alternative in modern construction, particularly for structures situated on soft to medium deposits (Chanda et al., 2020). The piled raft foundations are the foundation system that integrates the bearing capacity of the raft's base and piles to support loads of the structure. In contrast to the conventional design relying solely on piles, adopting the piled raft foundation concept can result in significant cost savings without compromising safety requirements. Initially, the piled raft foundation concept was introduced by adding piles below the raft foundation in cases where settlement exceeds the allowable limit (Burland et al., 1977; Poulos, 2001). Much research has been done on piled raft foundations under vertical loadings. While research on piled raft foundations has primarily focused on vertical loading conditions, investigations into their lateral resistance remain relatively limited. Most studies have contributed valuable insights into the lateral load response of piled raft foundations, predominantly under level ground conditions (Bhaduri and Choudhury, 2020; Horikoshi et al., 2003; Pastsakorn et al., 2002). It was concluded that the proportion of the horizontal load carried by raft in piled raft foundation was higher than that carried by piles at the initial loading stage. At larger displacements, the piles carried more load than the raft. The horizontal load proportion carried by the raft decreases as the pile head connections become less rigid (Matsumoto et al., 2010).

In addition to experimental studies, numerical analysis plays a pivotal role in understanding geotechnical problems in clayey soil (Chub-uppakarn et al., 2023; Hsiung et al., 2021; Likitlersuang et al., 2018b; Nguyen et al., 2022). The finite-element method is a powerful analytical technique gaining popularity for modeling construction projects (Likitlersuang et al., 2014). Recent research findings on numerical analysis have shed light on various aspects of soil behavior and foundation performance. Deb and Pal (2021) executed a series of laboratory experiments and finite element analyses of model piled raft foundations in silty clay and reported that the capacity of the piled raft and load sustained by the raft tends to increase with the increase of the vertical load. A similar conclusion was also reported by Bhaduri and Choudhury (2020), who studied the load-sharing and deformation behaviour of piled raft foundations using the finite element approach.

Only the piled raft systems in level ground conditions were assessed from the studies mentioned above. Due to the advantages of pile rafts over conventional pile group foundations, there are possibilities to provide more cost-efficient foundations when soil slopes need to be dealt with by adopting piled raft foundation concept. Therefore, the study attempts to assess the raft's contribution to load resistance and evaluate the feasibility of piled raft behavior near slopes. Thus, the present study focuses on the effect of slope on the lateral behaviors of piled raft foundations. Integrating numerical analysis into the study of geotechnical problems allows for a comprehensive examination of soil behavior and foundation performance. To examine the effects of soil slope on the lateral response of piled raft foundations, a series of 3D finite element analyses were conducted, referencing the case study of piled raft foundations with 3×3 steel pipe piles embedded in cohesive soil from the work of Nimityongskul et al. (2012).

2. FINITE ELEMENT MODELING

2.1 Numerical Model

The geometry of the problem analysed in the study is illustrated in Figure 1. The study adopted the characteristics of the problem, including slope angle, slope depth, pile section properties, and the soil profile from the full-scale lateral load tests reported by Nimityongskul et al. (2012). The analysis program includes piled raft and free-standing pile group foundations in level ground and near a slope condition at distances xD (Figure 1) of 0D, 2D, 4D, and 8D from the slope, with D representing the pile diameter.

The distinction between the piled raft and free-standing pile group models lies in the placement of the raft in the free-standing pile group, positioned 10 cm above the ground, to avoid contact with the ground surface. The soil slope was 2:1, having a depth of 2.7 m. The foundation comprised 3 × 3 steel pipe piles with an outer diameter of 0.3 m., and the wall thickness is 9.5 mm. Piles were arranged with a normal center-to-center spacing of 3 times pile diameters. The length of the pile was 8 m. The raft was 2.4 × 2.4 m concrete raft 0.8 m thick, as shown in Figure 1b.

Three-dimensional finite element analyses were performed using PLAXIS 3D. The model's validity was checked using the results of full-scale field lateral loading tests on a single pile near the slope and small-scale model laboratory tests of piled raft foundation. Figure 2 shows the geometry and finite element mesh of the piled raft foundation model in level ground and near the slope condition. The advantage of the symmetry across the x-axis was taken, and half of the model piled raft foundation and model ground were modeled to decrease the computation consumption.

2.2 Boundary Conditions

The dimensions of the soil mass were sufficiently large to render the effects of the model boundary insignificant. Several sensitivity tests were made to find the proper boundary size. A boundary greater than 20 times the pile diameter was found to have a negligible effect on the results. Hence, the horizontal side boundary and the vertical side boundary were kept at more than 20 times of the pile diameter. The boundary displacement condition of fully fixed was imposed to the bottom, and normally fixed was set on the vertical boundaries of the sides of the model geometry. In addition, a finer mesh size was used to model the soils near the structural elements, while a larger mesh size was used near the model boundary.

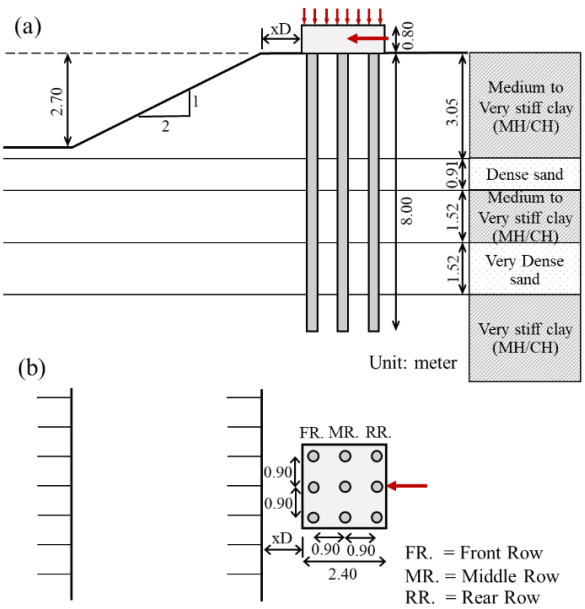

Figure 1 The problem geometry (a) elevation of the geometry (b) plan view of piled raft foundation

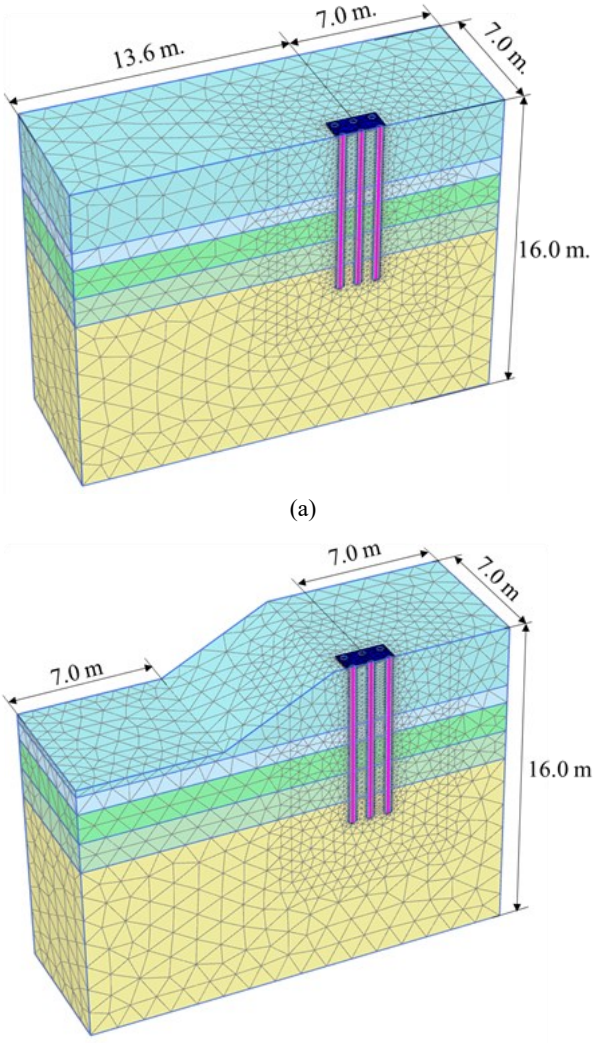

Figure 2 FEM mesh of piled raft foundation (a) in the level ground (b) near the slope condition

2.3 Material Modelling and Method of Analysis

Determining the list of soil parameters for laboratory and field testing requires considering the specific project's objectives and the soil type being investigated (Chompoorat and Likitlersuang, 2016; Chompoorat et al., 2021; Sukkarak et al., 2021). Reviewing relevant research on similar soils, like the studies focusing on Bangkok clays (Chompoorat et al., 2022; Likitlersuang et al., 2018a; Surarak et al., 2012). These studies typically present the soil parameters measured and their significance to the project's goals, such as understanding stiffness, strength, or behaviour under specific conditions (Likitlersuang et al., 2013a; Likitlersuang et al., 2013b). By analysing these studies and tailoring the parameters to your own project's needs, you can establish a comprehensive list of relevant soil properties for your laboratory and field-testing program (Julphunthong et al., 2018).

In this case, the soil ground was modelled by using 10-noded tetrahedral element. The Hardening soil model (HS-model) having parameters listed in Table 1 was adopted in the study. The HS-model parameters were determined by using soil investigation results (STP-N) and Mohr-Coulomb (MC) parameters reported by Nimityongskul et al. (2012) with correlations of the parameters and empirical value found in literatures (Bergado et al., 2022; Brinkgreve et al., 2022; Likitlersuang et al., 2019; Obrzud and Truty, 2018; Wu and Tung, 2020). Due to available undrained parameters, the Undrained B analysis, where strength is defined as undrained shear strength, was used for clay, and the Drained analysis was used for sand. The HS-model parameters were then validated with field test results, which will be discussed in Section 4.1.

Table 1 Material properties of the model ground

HS-model Parameters	Layer 1 Med. to V. stiff clay	Layer 2 Dense sand	Layer 3 Med. to V. stiff clay	Layer 4 V. dense sand	Layer 5 V. stiff clay
Depth of soil layer [m]	0-3.05	3.05-3.96	3.96-5.48	5.48-7.00	7-00-16.00
Unsaturated unit weight, γ_{unsat} [kN/m^3]	16.07	18.42	18.07	18.42	15.28
Saturated unit weight, γ_{sat} [kN/m^3]	18.07	20.42	20.07	20.42	17.28
Secant stiffness in standard drained triaxial test, E_{50}^{ref} [kN/m^2]	7565	28730	7565	30000	7565
Tangent stiffness for primary oedometer loading, E_{oed}^{ref} [kN/m^2]	7565	28730	7565	30000	7565
Unloading/reloading stiffness from drained triaxial test, E_{ur}^{ref} [kN/m^2]	22700	86190	22700	90000	22700
Poisson's ratio, ν_{ur} [-]	0.2	0.2	0.2	0.2	0.2
Undrained shear strength, $s_{u,ref}$ [kN/m^2]	90	0	114.9	0	167.6
Friction angle, φ ' [°]	0	40	0	42	0
Dilatancy angle, ψ [°]	0	10	0	12	0
Interface reduction factor, R_{inter} [-]	0.7	0.7	0.7	0.7	0.7

The raft was modeled through the plate element and meshed using 6-noded triangular element. The raft interface's reduction factor (Rinter) was 0.6 (Potyondy, 1961). The pile was modeled using hybrid elements, consisting of beam elements surrounded by solid elements, following the method described by Kimura and Zhang (2000) (Figure 3). In this method, the beam elements share a large portion of the pile's axial stiffness (EA) and bending stiffness (EI). However, the solid elements must be sufficiently rigid to represent the influence of pile size. The stiffness-sharing ratio between the beam and solid elements was 9 to 1. Adopting this hybrid modeling makes it easy to obtain the axial forces, bending moments, and shear forces of the pile based on the factored values of the beam elements. Although the piles were hollow cylinders, their properties were transformed to solid to model them as solid cylinder piles. The connection between the pile and the raft was rigid; consequently, the interface between the pile and the raft was omitted. Table 2 summarizes the beam pile, solid pile, and raft properties. After meshing, 35,640 elements, 59,986 nodes and total 37,742 elements, 63,155 nodes were generated for model in level ground and near a slope condition, respectively.

The modelling method was validated by small-scale laboratory test results of the piled raft foundation models in sand (Pastsakorn et al., 2002). The validation results will be discussed in Section 4.2.

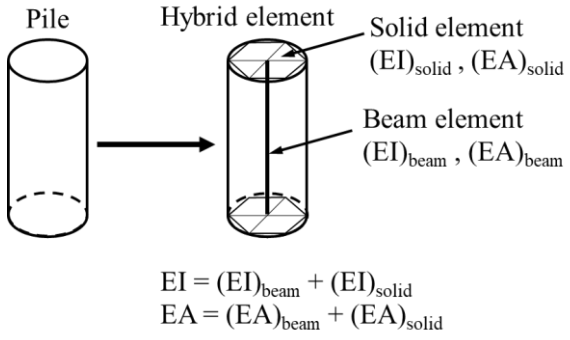

Figure 3 Hybrid pile element concept (after Kimura and Zhang, 2000)

Table 2 Material properties of the structural elements

Properties	Beam pile	Solid pile	Raft
Unit weight, γ [kN/m^3]	8.56	0.95	24
Elastic modulus, E [kN/m^2]	40.97 ×10^6	4.55 × 10^6	25 × 10^6
Poisson's ratio, ν [-]	-	0.3	0.2

3. THE ANALYSIS PROCEDURES

The following procedures were adopted in the FEM analysis.
Step 1: The initial stress state was calculated with the Ko-procedure, and the initial water condition was calculated using the phreatic level. No structural elements were activated during this calculation.
Step 2: The slope was created. The pile beam elements, raft plate elements, and interface elements were activated, and the properties of the solid pile element were changed to the pile properties. The self-weight of structural elements was also considered in this calculation.
Step 3: Calculation of loading process. The vertical load was first applied to the foundation before lateral loading. The vertical load was $0.5V_u$, where V_u is the ultimate vertical capacity defined as the load corresponding to 0.1D settlement. The lateral loading of the model was performed in a displacement-controlled manner. The lateral displacement was increased by 2D interval until 20D displacement was reached.

4. COMPARISON AND VALIDATION OF THE MODEL

The FEM models of piled raft foundations were validated through the two case studies. The objective of the first case study was to validate the HS-model parameters using the results of the full-scale lateral load test of piles near a slope reported by Nimityongskul et al. (2012). The second case study aimed to validate piled raft models created in PLAXIS 3D with the small-scale model laboratory test results published by Pastsakorn et al. (2002). The following Sections describe the two case studies in greater detail.

4.1 Full-Scale Lateral Load Test of the Pile Near a Slope

Nimityongskul et al. (2012) conducted a series of full-scale lateral tests of fully instrumented piles in cohesive and cohesionless soils to assess the lateral response of piles near a slope condition. However, only cohesive soil is interested in the present study. The HS model

was adopted in the present study instead of the initially proposed MC model. The HS-model properties are present in Table 1. The single piles were modeled with the same method as piles in piled raft foundations. The comparative results are shown in Figure 4.

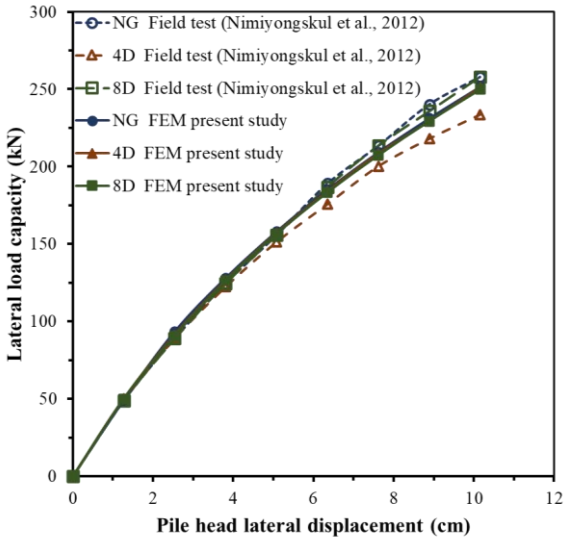

Figure 4 Displacement curve for comparison

A good compatibility could be observed between the full-scale lateral load test and FEM analysis in the case of a pile at the distance 8D from a slope and a pile in level ground (NG). For a pile at a distance 4D from a slope, the FEM overestimates the lateral capacity at large displacement. This is because, at large displacement, the loosening of soil particles occurring at a slope causes a reduction in lateral resistance, which FEM cannot simulate this effect. However, the maximum applied displacement in the present study was 20D or 6 cm. The results show good agreement within this range.

4.2 Small-Scale Model Laboratory Test

Pastsakorn et al. (2002) executed lateral load tests on pile group and piled raft foundation models in Toyoura sand under 1g field condition. The Toyoura sand was prepared in an acrylic box with dimensions of 500 mm in width and 840 mm in length. The raft models were made of duraluminium plates with a thickness of 22 mm, Young's modulus is 68,670 MN/m, and Poisson's ratio is 0.335. The piles were made of aluminum pipe having an outer diameter of 20 mm and a wall thickness of 1 mm. The length of the piles is 200 mm. Young's modulus and Poisson's ratio are 70,632 and 0.245, respectively. The raft size, number of piles, and pile spacing were varied in the study. The pile raft case with the raft size of 225 mm × 225 mm, having four piles and piles spacing of 150 mm, was selected to validate the FEM model. The piled raft in FEM was modelled in the same manner as described in Section 2. The sand ground model throughout the analysis employed the HS model. The material properties of Toyoura sand, based on the HS model, were previously documented by Ashour and ÜNsever (2022).

The comparison between experimental results and FEM analysis of the present study shows a good agreement, as shown in Figure 5. A similar trend of the displacement curves is observed for both piled raft (total lateral capacity) and pile components. The comparison proves the correctness of the modelling method.

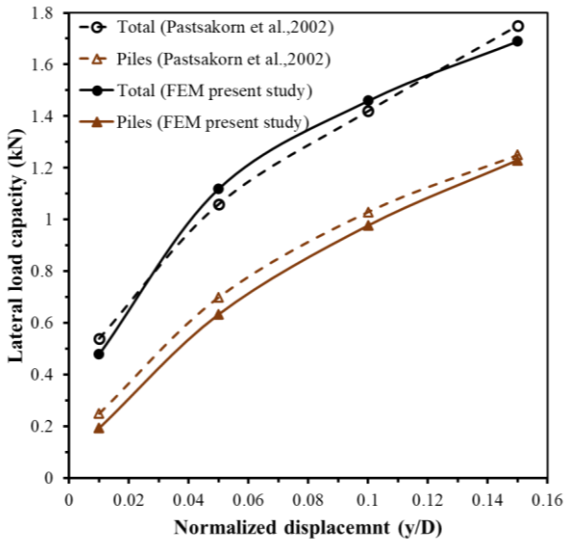

Figure 5 Displacement curve comparison between small-scale model test and FEM

5. RESULTS AND DISCUSSIONS

5.1 Piled Raft Foundation in Level Ground

The results of the piled raft and pile group foundations on the level ground served as a baseline result for piled raft foundations near a slope condition. During vertical loading on the piled raft, the raft was observed to share 16.5% of the vertical load applied before lateral loading. The lateral load at each lateral displacement target was normalized in terms of $F_L/(S_uD^2)$ to make the results easier to visualize and interpret, where F_L is the lateral force, S_u is the undrained shear strength, and D is the diameter of the pile. Normalization was conducted using the undrained shear strength of the first clay layer because it is the most influential layer and enables the obtaining of unitless results. Lateral displacement was normalized in terms of y/D, where y is the lateral displacement. Figure 6 displays the lateral response of a piled raft and its components (raft and piles) compared to the free-standing pile group's lateral response.

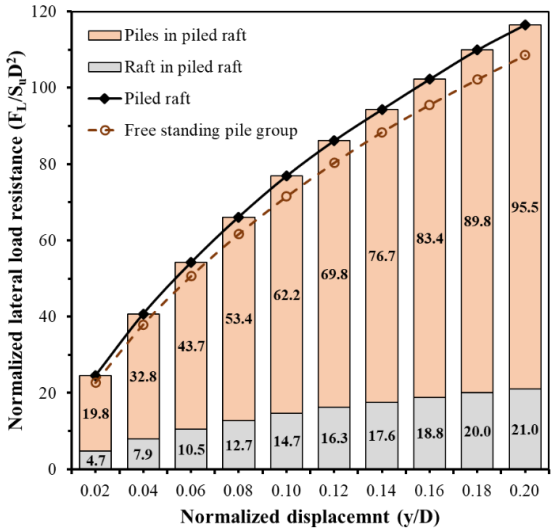

Figure 6 Lateral response of piled raft and pile group foundation in level ground

At a normalized displacement of 0.1, the overall lateral capacity of a piled raft is 7.0% greater than that of a free-standing pile group. Comparing the load proportion taken by piles in a piled raft to the free-standing pile group capacity, the lateral load taken by piles in a piled raft is 12.0% less than that of the free-standing pile group (at a

normalized displacement of 0.1). This is because, in the case of a free-standing pile group, the lateral loads are entirely supported by the piles, whereas in the case of a piled raft, the lateral loads are shared between the raft and the piles. Figure 7 illustrates the proportion of lateral load the raft carries as a function of normalized displacement. It revealed that the raft carried less lateral load as displacement increased. The raft shares 19.4% of the lateral load at the beginning of the displacement, then the lateral load shared by the raft decreases to 18.0% as the normalized displacement increases to 0.20.

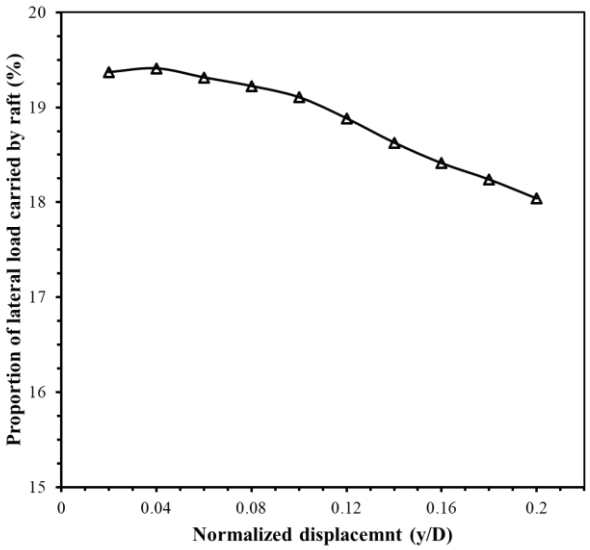

Figure 7 Proportion of lateral load carried by raft of piled raft foundation in level ground

5.2 Piled Raft Foundation Near a Slope Condition

FEM analyses were conducted on model piled raft foundations at distances of 0D, 2D, 4D, and 8D from the slope crest. The vertical load-sharing ratio appears unaffected by a slope, as the raft maintains the sharing ratio of 16.38% of the total vertical load (applied before lateral loading). However, further parametric studies need to be done to fully comprehend the effect of slope on the vertical response of a piled raft foundation. The lateral response of a piled raft foundation near a slope is depicted in Figure 8.

At the distance 8D from the slope crest, the lateral displacement of the piled raft foundation is approximately the same as in the level ground, indicating that the slope no longer affects the behavior of piled raft foundations at this location, which agrees with the conclusion reported in the case of the single pile (Nimityongskul et al., 2012). As the locations of the piled raft foundations get closer to the slope, the maximum lateral capacity decreases gradually. Although the initial stiffness is similar for all piled raft cases. But, at greater displacement, for example, at y/D = 0.1, the capacity of piled rafts at 4D, 2D, and 0D from the slope crest decreased by 3.0%, 6.5%, and 10.0%, respectively. When compared to the results of the full-scale lateral load test on single piles (Nimityongskul et al., 2012), the lateral capacity of single piles decreased by 3.5%, 7.14%, and 21.4% when the distances changed from 8D to 4D, 2D, and 0D from the slope crest, respectively. The reduction in the lateral capacity of 4D and 2D piled rafts is compatible with the full-scale lateral load test on a single pile. However, for the 0D piled raft, it seemed to be 2 times less. In fact, in the case of the 0D piled raft, the center of the front row piles was located 1D away from the slope crest (the edge of the raft extended 1D from the center of the outer piles), while the center of single pile locates at the slope crest. Thus, the 10% decrease in lateral capacity is reasonable.

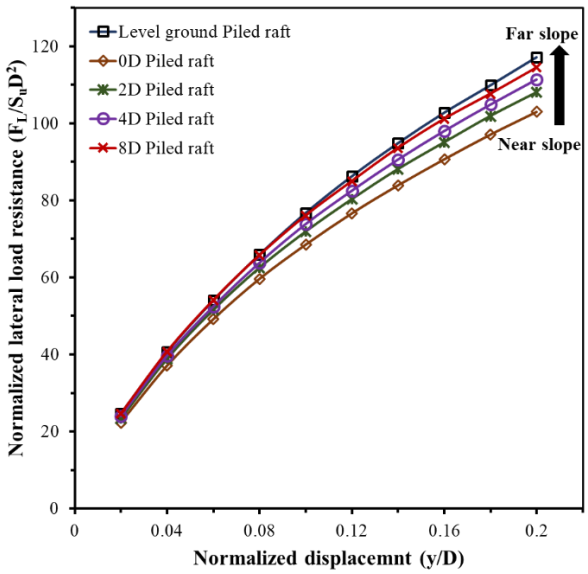

Figure 8 Lateral response of piled foundation near a slope

Figure 9 compares the lateral load sharing ratio on the raft. At distances greater than 2D, the contribution of the raft is approximately the same when the normalized displacement (y/D) is lower than 0.14. However, at larger displacement, the load sharing ratio of rafts in 8D piled raft and piled raft in level ground decrease rapidly compared to 4D and 2D piled raft. As the 8D piled raft and piled raft in level ground possess stronger pile capacity than 2D and 4D cases, the lateral load tends to transfer to the piles. The raft's load-sharing ratio is significantly reduced in the 0D piled raft. The reduction results from the diminishing contact pressure at the raft-soil interface. The average contact pressure at the interface of the 8D piled raft is 49.89 kN/m^2, while for the 0D piled raft, it is 46.5 kN/m^2 as shown in Figure 10.

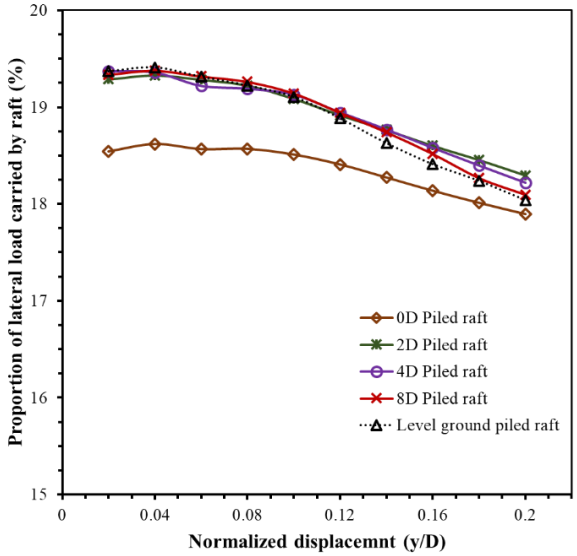

Figure 9 Lateral load sharing ratio of the raft in piled raft foundations near a slope condition

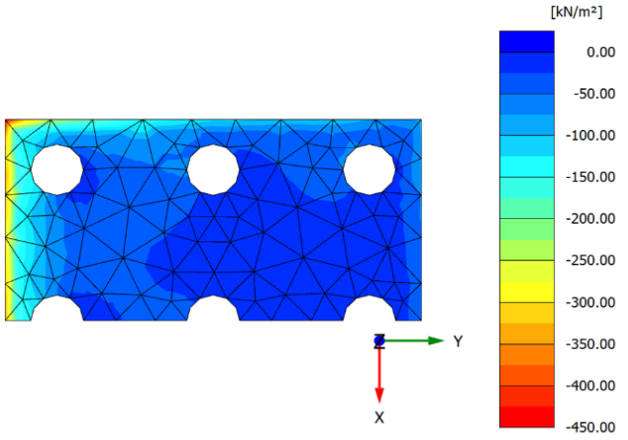

(a)

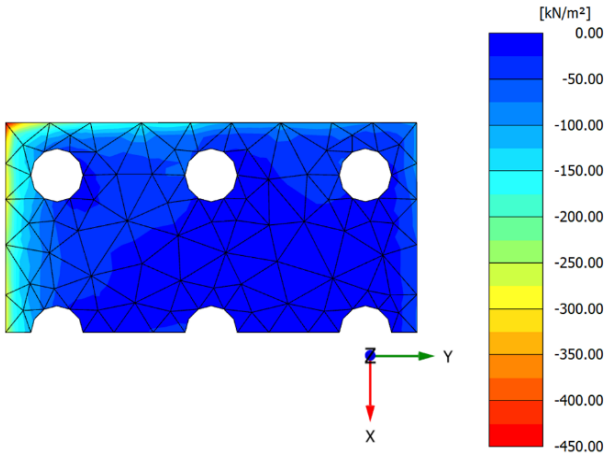

(b)

Figure 10 Contact pressure in raft – soil interface when y/D = 0.1 (a) 8D piled raft (b) 0D piled raft

Figure 11 shows the overall lateral capacity of pile and raft in the piled raft system focused on lateral displacement (y/D) of 0.1 and 0.2. As mentioned earlier, at the distance 8D and beyond, the slope effect is almost negligible. At distances between 8D and 4D, the lateral capacity of the pile gradually decreases. The pile's rapid decrease in the lateral capacity is observed at a distance closer than 2D. While raft capacity remains approximately constant until at the distances 2D from the slope. The decrease in lateral capacity of the raft is observed at distances closer than 2D.

Comparing the lateral capacity of the piled raft and free-standing pile group foundation at 0D from the slope crest, as shown in Figure 12, the piled raft shows a higher lateral capacity, around 7.0%, than the pile group. When considering the lateral load carried by pile components within the piled raft, the load distributed to the piles is 12.8% lower than the total lateral load carried by the free-standing pile group (at a normalized displacement of 0.1). The results indicate that adopting the piled raft foundation concept offers two significant advantages: an increase in overall lateral capacity and a reduction in the lateral load transferred to the piles.

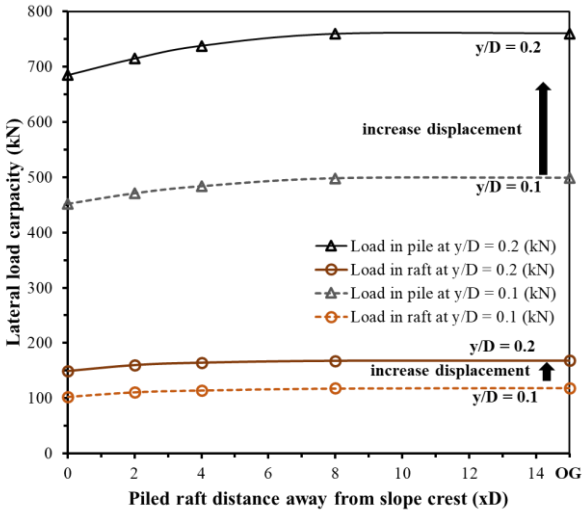

Figure 11 The effect of the distance of the slope crest on lateral capacity of pile and raft in piled raft system

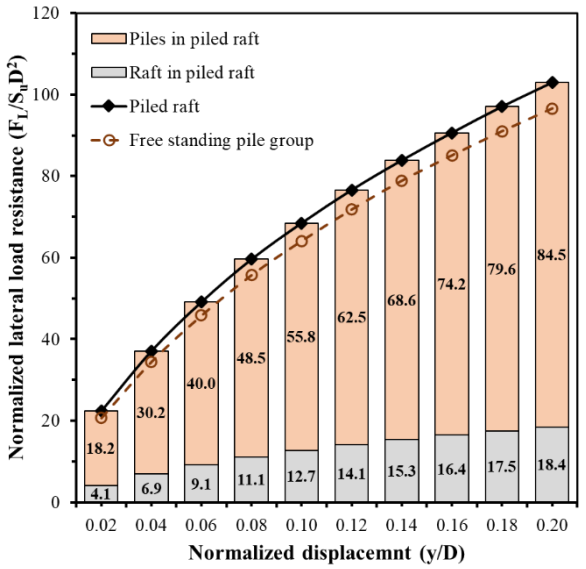

Figure 12 Lateral response of piled raft and free – standing pile group at the distance 0D from the slope crest

Figure 13 shows the bending moment along the shaft of the front and rear row piles. Piles in the front row take a higher lateral load than piles in the rear row, as shown in Figures 13(a) and 13(b). The distance from the crest of the slope has a significant impact on the front row pile than the rear row piles, as shown in Figure 14. The maximum negative moment of the front row pile decreases by 6.60% when the distance changes from 8D to 0D from the slope, while the rear pile maintains a similar value. It can be concluded that the loss in lateral capacity of the piled raft systems when they are constructed near the slope occurs due to the loss in lateral capacity of the front piles.

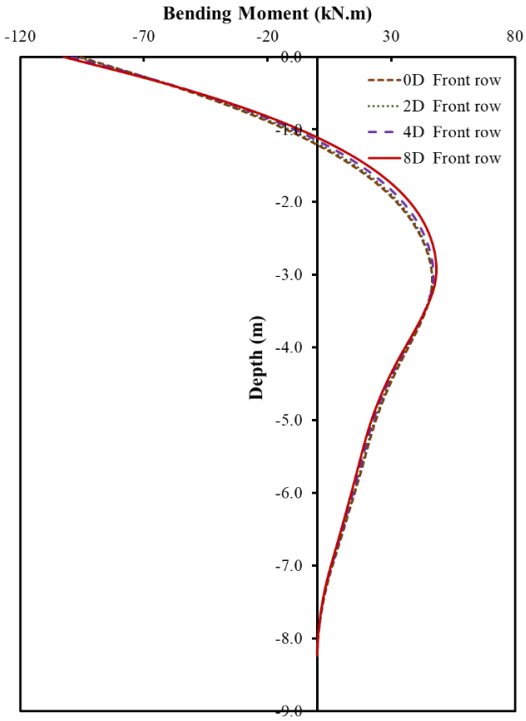

(a)

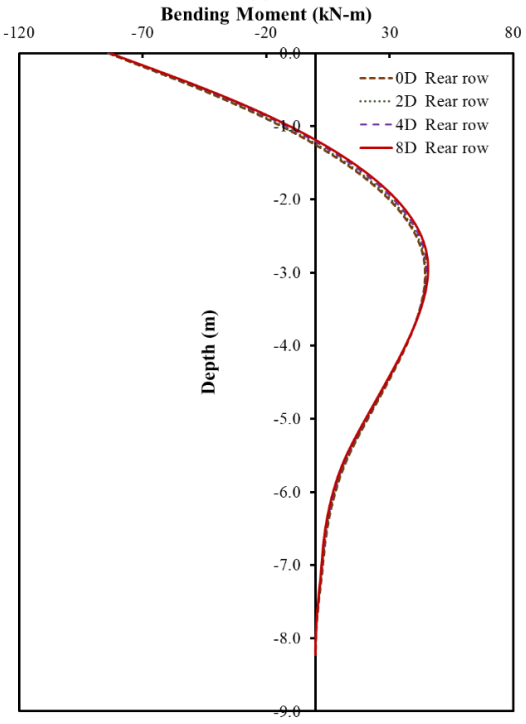

(b)

Figure 13 Bending moment along the pile shaft (a) Front row pile, (b) Rear row pile

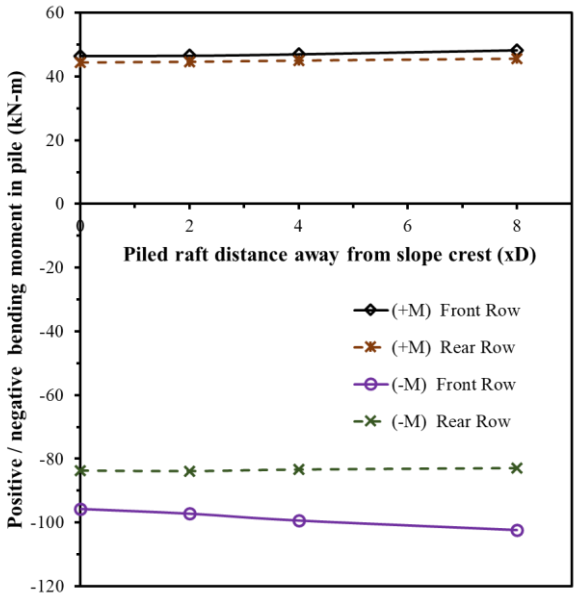

Figure 14 Comparison of maximum and minimum moment in the pile shaft between the front piles and the rear piles

5.3 The Mechanism Behind the Response of the Piled Raft Foundation System Near the Slope

The mechanism behind the response of the piled raft foundation system near the slope is elucidated in Figures 15 and 16. Figure 15 illustrates the mobilized shear stress (τ_{mod}) in the soil mass. When subjected to lateral loading, for the piled raft system at 8D from the slope crest, the mobilized stress does not reach the slope, as shown in Figure 15a. At 0D, the mobilized shear stress is observed on the slope, as shown in Figure 15b. The failure wedge extends up to the slope. The lower passive resistance at the slope causes a reduction in the lateral capacity of the piled raft systems. Figure 16 shows the failure wedge of the piled raft foundation near the slope.

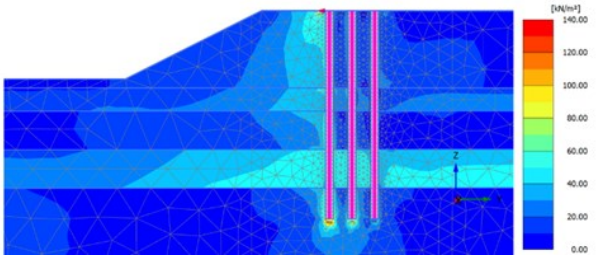

(a)

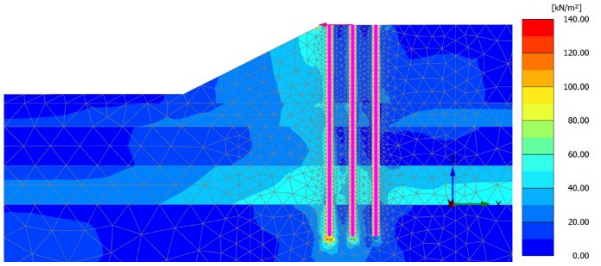

(b)

Figure 15 The mobilized shear stress (τ_{mod}) in the soil mass (a) 8D piled raft (b) 0D piled raft

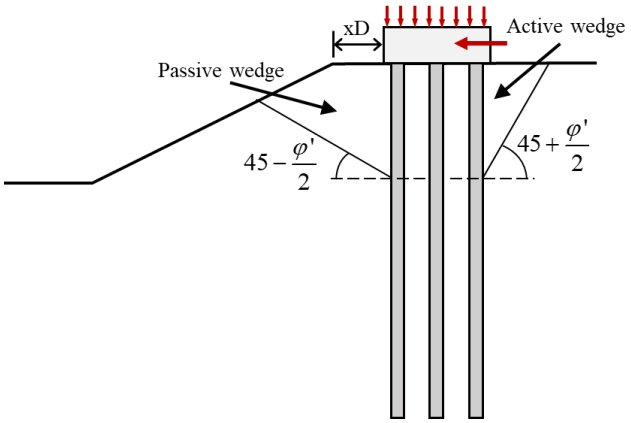

Figure 16 The failure mechanism of the piled raft foundation system near the slope

6. CONCLUSIONS

The FEM analyses were carried out using the finite element analysis to investigate the effects of soil slope on the lateral response of piled raft foundation system. The case study was a 2.4 × 2.4 × 0.8 m piled raft foundation on medium stiff clay ground. The piles were 9 steel pipe piles with an outer diameter of 0.3 m arranged with piles spacing 3 times the pile diameter. The analysis program covered piled raft foundations and free-standing piled group foundations in level ground and near the slope crest to compare the results. The main findings can be summarized as follows:

1. The slope affects the response of piled raft foundations when they are installed at certain distance less than 8 times of pile diameter (8D) in which lateral capacity of piled raft foundation deceases. The enormous effect of slope can be observed within the distances closer than 4D when the lateral capacity decreases rapidly. In additional, the slope tends to affect only the front piles rather than the rear piles.

2. Piled raft foundations offer higher lateral capacity than the pile group. The critical factor is the interaction between the raft and the pile. The raft increases the lateral capacity of piled raft foundations while reducing lateral load transfer to piles.

3. A slope insignificantly affects the proportion of the lateral load sharing by the raft component, especially at a distance greater than 2D. It shows the advantages of the piled raft foundation over the pile group when foundations need to be constructed near a slope. However, at a distance closer than 2D, the load-sharing ratio tends to be affected by a slope due to the loss of passive resistance and the loosening of soil particles at the slope, which reduces the efficiency of piled raft foundations.

4. In conclusion, the distance between the piled raft foundation and a slope plays important rule and need to be considered to improve design guidance which would lead to economical design without compromising safety requirement.

7. ACKNOWLEDGMENTS

This research is supported by Prince of Songkla University and the National Research Council of Thailand (Grant N0. ENG6601099S) and by the National Research Council of Thailand Research and Innovation Fund and the University of Phayao (Grant N0. 231/2567). The authors sincerely thank Prince of Songkla University and Southern Natural Disaster Research Center for providing us with great support and resources in completing this study. We are grateful for their generous funding enabling us to conduct our study and complete this research.

8. REFERENCES

Ashour, S., and ÜNsever, Y. S. (2022). "Static Analyses of the Effect of Deep Excavation on the Behaviour of an Adjacent Pile in Sand." *Uludağ Üniversitesi Mühendislik Fakültesi Dergisi,* 27(2), 627-646. https://doi.org/10.17482/uumfd.971609.

Bergado, D. T., Jamsawang, P., Jongpradist, P., Likitlersuang, S., Pantaeng, C., Kovittayanun, N., and Baez, F. (2022). "Case Study and Numerical Simulation of PVD Improved Soft Bangkok Clay with Surcharge and Vacuum Preloading using a Modified Air-Water Separation System." *Geotextiles and Geomembranes,* 50(1), 137-153. https://doi.org/https://doi.org/10.1016/j.geotexmem.2021.09.009.

Bhaduri, A., and Choudhury, D. (2020). "Serviceability-Based Finite-Element Approach on Analyzing Combined Pile–Raft Foundation." *International Journal of Geomechanics,* 20(2), 04019178. https://doi.org/10.1061/(ASCE)GM.1943-5622.0001580.

Brinkgreve, R. B. J., Kumarswamy, S., Swolfs, W. M., and Fonseca, F. (2022). "Plaxis 3D 2022 Manual." *Plaxis Company.*

Burland, J., Broms, B., and Mello, V. (1977). "Behaviour of Foundations and Structures."

Chanda, D., Saha, R., and Haldar, S. (2020). "Behaviour of Piled Raft Foundation in Sand Subjected to Combined V-M-H Loading." *Ocean Engineering,* 216, 107596. https://doi.org/10.1016/j.oceaneng.2020.107596.

Chompoorat, T., and Likitlersuang, S. (2016). "Assessment of Shrinkage Characteristic in Blended Cement and Fly Ash Admixed Soft Clay." *Japanese Geotechnical Society Special Publication,* 2(6), 311-316. https://doi.org/10.3208/jgssp.THA-01.

Chompoorat, T., Likitlersuang, S., Sitthiawiruth, S., Komolvilas, V., Jamsawang, P., and Jongpradist, P. (2021). "Mechanical Properties and Microstructures of Stabilised Dredged Expansive Soil from Coal Mine." *Geomechanics and Engineering,* 25(2), 143. https://doi.org/10.12989/gae.2021.25.2.143.

Chompoorat, T., Thepumong, T., Khamplod, A., and Likitlersuang, S. (2022). "Improving Mechanical Properties and Shrinkage Cracking Characteristics of Soft Clay in Deep Soil Mixing." *Construction and Building Materials,* 316, 125858. https://doi.org/10.1016/j.conbuildmat.2021.125858.

Chub-uppakarn, T., Chompoorat, T., Thepumong, T., Sae-Long, W., Khamplod, A., and Chaiprapat, S. (2023). "Influence of Partial Substitution of Metakaolin by Palm Oil Fuel Ash and Alumina Waste Ash on Compressive Strength and Microstructure in Metakaolin-Based Geopolymer Mortar." *Case Studies in Construction Materials,* 19, e02519. https://doi.org/10.1016/j.cscm.2023.e02519.

Deb, P., and Pal, S. K. (2019). "Numerical Analysis of Piled Raft Foundation under Combined Vertical and Lateral Loading." *Ocean Engineering,* 190, 106431. https://doi.org/10.1016/j.oceaneng.2019.106431.

Deb, P., and Pal, S. K. (2021). "Nonlinear Analysis of Lateral Load Sharing Response of Piled Raft Subjected to Combined V-L Loading." *Marine Georesources & Geotechnology,* 39(8), 994-1014. https://doi.org/10.1080/1064119X.2020.1766607.

Georgiadis, K., and Georgiadis, M. (2010). "Undrained Lateral Pile Response in Sloping Ground." *Journal of Geotechnical and Geoenvironmental Engineering,* 136(11), 1489-1500. https://doi.org/10.1061/(ASCE)GT.1943-5606.0000373.

Horikoshi, K., Matsumoto, T., Hashizume, Y., Watanabe, T., and Fukuyama, H. (2003). "Performance of Piled Raft Foundations Subjected to Static Horizontal Loads." *International Journal of Physical Modelling in Geotechnics,* 3(2), 37-50. https://doi.org/10.1680/ijpmg.2003.030204.

Hsiung, B.-C. B., Likitlersuang, S., Phan, K. H., and Pisitsopon, P. (2021). "Impacts of the Plane Strain Ratio on Excavations in Soft Alluvium Deposits." *Acta Geotechnica,* 16(6), 1923-1938. https://doi.org/10.1007/s11440-020-01115-3.

Jamsawang, P., Voottipruex, P., Jongpradist, P., and Likitlersuang, S. (2021). "Field and Three-Dimensional Finite Element

Investigations of the Failure Cause and Rehabilitation of a Composite Soil-Cement Retaining Wall." *Engineering Failure Analysis,* 127, 105532. https://doi.org/10.1016/j.engfailanal.2021.105532.

Jiang, C., He, J.-L., Liu, L., and Sun, B.-W. (2018). "Effect of Loading Direction and Slope on Laterally Loaded Pile in Sloping Ground." *Advances in Civil Engineering,* 2018, 7569578. https://doi.org/10.1155/2018/7569578.

Julphunthong, P., Thongdetsri, T., and Chompoorat, T. (2018). "Stabilization of Soft Bangkok Clay using Portland Cement and Calcium Sulfoaluminate-Belite Cement." *Key Engineering Materials,* 775, 582-588. https://doi.org/10.4028/www.scientific.net/KEM.775.582.

Kimura, M., and Zhang, F. (2000). "Seismic Evaluations of Pile Foundations with Three Different Methods Based on Three-Dimensional Elasto-Plastic Finite Element Analysis." *Soils and Foundations,* 40(5), 113-132. https://doi.org/10.3208/sandf.40.5_113.

Likitlersuang, S., Chheng, C., and Keawsawasvong, S. (2019). "Structural Modelling in Finite Element Analysis of Deep Excavation." *Journal of GeoEngineering,* 14(3), 121-128. https://doi.org/10.6310/jog.201909_14(3).1.

Likitlersuang, S., Chheng, C., Surarak, C., and Balasubramaniam, A. (2018a). "Strength and Stiffness Parameters of Bangkok Clays for Finite Element Analysis." *Geotechnical Engineering,* 49.

Likitlersuang, S., Pholkainuwatra, P., Chompoorat, T., and Keawsawasvong, S. (2018b). "Numerical Modelling of Railway Embankments for High-Speed Train Constructed on Soft Soil." *Journal of GeoEngineering,* 13(3), 149-159. https://doi.org/10.6310/jog.201809_13(3).6.

Likitlersuang, S., Surarak, C., Suwansawat, S., Wanatowski, D., Oh, E., and Balasubramaniam, A. (2014). "Simplified Finite-Element Modelling for Tunnelling-Induced Settlements." *Geotechnical Research,* 1(4), 133-152. https://doi.org/10.1680/gr.14.00016.

Likitlersuang, S., Surarak, C., Wanatowski, D., Oh, E., and Balasubramaniam, A. (2013a). "Geotechnical Parameters from Pressuremeter Tests for MRT Blue Line Extension in Bangkok." *Geomechanics and Engineering,* 5, 99-118. https://doi.org/10.12989/gae.2013.5.2.099.

Likitlersuang, S., Teachavorasinskun, S., Surarak, C., Oh, E., and Balasubramaniam, A. (2013b). "Small Strain Stiffness and Stiffness Degradation Curve of Bangkok Clays." *Soils and Foundations,* 53(4), 498-509. https://doi.org/10.1016/j.sandf.2013.06.003.

Matsumoto, T., Nemoto, H., Mikami, H., Yaegashi, K., Arai, T., and Kitiyodom, P. (2010). "Load Tests of Piled Raft Models with Different Pile Head Connection Conditions and Their Analyses." *Soils and Foundations,* 50(1), 63-81. https://doi.org/10.3208/sandf.50.63.

Mezazigh, S., and Levacher, D. (1998). "Laterally Loaded Piles in Sand: Slope Effect on P-Y Reaction Curves." *Canadian Geotechnical Journal,* 35(3), 433-441. https://doi.org/10.1139/t98-016.

Nguyen, T. S., Phan, T. N., Likitlersuang, S., and Bergado, D. T. (2022). "Characterization of Stationary and Nonstationary Random Fields with Different Copulas on Undrained Shear Strength of Soils: Probabilistic Analysis of Embankment Stability on Soft Ground." *International Journal of Geomechanics,* 22(7), 04022109. https://doi.org/10.1061/(ASCE)GM.1943-5622.0002444.

Nimityongskul, N., Barker, P. D., Ashford, S. A., Infrastructure, K. C. f., and Transportation. (2012). "Effects of Soil Slope on Lateral Capacity of Piles in Cohesive and Cohesionless Soils." *Structure Policy and Innovation,* California Department of Transportation, Division of Engineering Services.

Nimityongskul, N., Kawamata, Y., Rayamajhi, D., and Ashford, S. A. (2018). "Full-Scale Tests on Effects of Slope on Lateral Capacity of Piles Installed in Cohesive Soils." *Journal of Geotechnical and Geoenvironmental Engineering,* 144(1), 04017103. https://doi.org/10.1061/(ASCE)GT.1943-5606.0001805.

Obrzud, R., and Truty, A. (2018). "The Hardening Soil Model : A Practical Guidebook." Zace Services Lausanne.

Pastsakorn, K., Hashizume, Y., and Matsumoto, T. (2002). "Lateral Load Tests on Model Pile Groups and Piled Raft Foundations in Sand." *In Proceedings of the International Conference Physical Modelling in Geotechnics*, 709-714.

Potyondy, J. G. (1961). "Skin Friction between Various Soils and Construction Materials." *Géotechnique,* 11(4), 339-353. https://doi.org/10.1680/geot.1961.11.4.339.

Poulos, H. G. (2001). "Piled Raft Foundations: Design and Applications." *Géotechnique,* 51(2), 95-113. https://doi.org/10.1680/geot.2001.51.2.95.

Sukkarak, R., Likitlersuang, S., Jongpradist, P., and Jamsawang, P. (2021). "Strength and Stiffness Parameters for Hardening Soil Model of Rockfill Materials." *Soils and Foundations,* 61(6), 1597-1614. https://doi.org/10.1016/j.sandf.2021.09.007.

Surarak, C., Likitlersuang, S., Wanatowski, D., Balasubramaniam, A., Oh, E., and Guan, H. (2012). "Stiffness and Strength Parameters for Hardening Soil Model of Soft and Stiff Bangkok Clays." *Soils and Foundations,* 52(4), 682-697. https://doi.org/10.1016/j.sandf.2012.07.009.

Wu, J. T. H., and Tung, S. C.-Y. (2020). "Determination of Model Parameters for the Hardening Soil Model." *Transportation Infrastructure Geotechnology,* 7(1), 55-68. https://doi.org/10.1007/s40515-019-00085-8.